ELSEVIER

Biochimica et Biophysica Acta 1467 (2000) 18–26

BIOCHIMICA ET BIOPHYSICA ACTA
BBA

www.elsevier.com/locate/bba

Formation and characterization of phosphatidylethanolamine/lysophosphatidylcholine mixed vesicles

Changqui Sun, Aya Hanasaka, Hiroshi Kashiwagi, Masaharu Ueno *

Faculty of Pharmaceutical Sciences, Toyama Medical and Pharmaceutical University, 2630 Sugitani, Toyama 930-0194, Japan

Received 12 October 1999; received in revised form 28 February 2000; accepted 14 March 2000

Abstract

The lipid aggregates formed by adding lysophosphatidylcholine (lysoPC) solution to phosphatidylethanolamine (PE) dispersion at 4°C followed by incubating it at 37°C were proved to be a vesicle system judged from the negatively stained electron micrographs and the latency of calcein fluorescence. The results obtained are analogous to those described for phosphatidylcholine (PC) vesicles. The chromatography results showed that the incorporation of PE and lysoPC into the PE/lysoPC vesicles was in a molar ratio of 5 to 2. The PE/lysoPC membrane was found to have similar barrier potentials for Cl^- or calcein efflux to the PC membrane. ^1H Nuclear magnetic resonance measurement suggested that lysoPC dominated the external monolayer of the vesicles. Furthermore, it was found that PE/lysoPC vesicles and micelles could coexist when a large amount of lysoPC was added to the PE/lysoPC vesicle suspension. The formation of PE/lysoPC vesicles is discussed in combination with the inhibition of interlayer attachment by lysoPC from the PE membrane.

Keywords: Phosphatidylethanolamine; Lysophosphatidylcholine; Vesicle; Barrier potential; Gel chromatography; Nuclear magnetic resonance

1. Introduction

The lipid aggregates and their functions are sensitive to geometric considerations such as the molecular shapes as well as thermodynamic factors. This has also led to a possible rationale for lipid diversity in the membrane in terms of the phase behaviors for lipids with a variety of shapes [1,2]. Phosphatidylethanolamine (PE) has been reported to have a cone shape and form a lamellar phase at low temperature and a H_{II} phase under physiological conditions [3,4]. For the lamellar (L_α) to nonlamellar (H_{II}) phase transition of PE, inverted micellar intermediate (IMI) structures play a pivotal role in interlamellar attachments (ILA) leading to H_{II} formation [5,6]. The interaction of PE lipids in the target membrane and other fusion factors, including fusion proteins or peptides, forms an intermediate stalk structure [7]. The stalk structure has a net negative curvature [8,9]. The IMI or stalk may promote vesicle–vesicle or vesicle–virus fusion as a fusion intermediate [10–12]. This is due to the negative curvature of a monolayer in the H_{II} phase. Lipids, such as PE, that can form a H_{II} phase or promote its formation are considered to have a negative spontaneous curvature in the membrane [13,14].

In contrast, lysophosphatidylcholine (lysoPC) has an inverted cone shape and prefers a micellar orga-

* Corresponding author. Fax: +81-76-434-5050; E-mail: mueno@ms.toyama-mpu.ac.jp

0005-2736/00/$ – see front matter
PII: S0005-2736(00)00192-9

nization in excess water. Micelle-forming lipids possess a positive spontaneous curvature [15]. Although lysoPC caused lysis and cell fusion [16], it was recently found to inhibit the formation of stalks at a low concentration, including the stalk induced by the fusogenic peptides [17,18]. The effect of lysoPC on the stalks themselves could be different, but the larger head-group of lysoPC than the tail diameter could make lysoPC present in the outer leaflet of the membrane, blocking the formation of negative curvature [2]. Therefore, the inhibition of the stalk by lysoPC would be a dynamic complementary behavior of the molecular shapes.

In this paper, we studied PE/lysoPC vesicles based on the shape complementarity of PE and lysoPC. Formation of the PE/lysoPC vesicles was first confirmed by observing the morphology and entrapment efficiency. Further, their barrier potentials as well as the lysoPC behaviors in the bilayer were investigated using electron microscopy, fluorescence and nuclear magnetic resonance (NMR) spectroscopy. The comparison with phosphatidylcholine (PC) vesicles made us learn something about the characterized PE/lysoPC bilayer. We will focus here on the effect of the molecular packing of the membrane on the behaviors of the PE/lysoPC membrane. The results will help us observe further the inhibition of vesicle fusion or stalk structure by lysoPC.

2. Materials and methods

2.1. Materials

PE and lysoPC isolated from egg yolk were purchased from Sigma (St. Louis, MO, USA). Lecithin (egg PC) was obtained from Nihon Yushi (Tokyo, Japan). Calcein, praseodym nitrate hexahydrate, *N*-tris(hydroxymethyl)methyl-2-aminoethanesulfonic acid (TES) and other reagents were purchased from Nacalai Tesque (Kyoto, Japan).

2.2. Preparation of the vesicle suspensions

Multilamellar vesicles (MLV) of PE/lysoPC were prepared as follows: PE was dispersed in a calcein solution (150 mM NaCl, 10 μM calcein and 20 mM TES, pH 7.0) at 4°C by vortexing, then after lysoPC solution was added, the suspensions of PE and lysoPC were incubated for 2 h at 37°C. PC MLV was prepared by dispersing dried PC film into the same buffer solution with vortexing. In order to prepare the extruded vesicles, the PE/lysoPC MLVs were frozen and thawed five times, then extruded through two stacked 0.6 μm defined or 0.2 μm defined pore polycarbonate filters (Nucleopore, Costar Co., USA) at least five times. Small unilamellar vesicles (SUV) were prepared by ultrasonication with a ultrasonic generator (US-600TS, Nissei, Japan). The MLV suspension of 4 ml × 25 mM phospholipids was ultrasonicated three times for 20 min, with a rest time of 10 min, at ice-bath temperature and under a nitrogen atmosphere. Titanium fragments and multilamellar aggregates were removed by centrifugation at $100\,000 \times g$ for 60 min at 4°C. Here, SUV were found to have a uniform size. The mean diameter and size distribution of the vesicles were determined by quasielastic light scattering using an LPA3000/3100 laser particle analyzer (Otsuka Electronics, Japan). Electron microscopy (EM) was performed on a JEM-200 microscopy (JEOL, Japan). The EM samples observed were prepared with 2% potassium phosphotungstate for staining.

2.3. Calcein entrapment efficiency measurement

The calcein entrapment efficiency of the vesicles was determined according to Oku et al. [19]. The vesicles were prepared in 10 μM of a calcein solution; the remaining fluorescence intensities were measured after the fluorescence of untrapped calcein was quenched by the addition of an appropriate amount of 100 mM $CoCl_2$. The fluorescence intensity of a sample was recorded continuously subsequent to this dilution (zero time) on an RF-500 fluorescence spectrophotometer (Shimadzu, Japan) (excitation $\lambda = 490$ nm, emission $\lambda = 520$ nm) equipped with temperature control accessories and a magnetic stirrer. The entrapment efficiency was calculated by the following equation:

$$\text{entrapment efficiency (\%)} = 100 \times (f_{\text{in}\cdot r1} - f_{\text{total.q}\cdot r2}) / (f_{\text{total}} - f_{\text{total.q}\cdot r2}) \quad (1)$$

where f_{in} is the fluorescence intensity of the internal calcein; f_{total} and $f_{\text{total.q}}$ are the total fluorescence in-

tensity of calcein before and after vesicle destruction, respectively; $r1$ and $r2$ are correction factors for the volume increase upon adding a $CoCl_2$ solution and the Triton X-100 solution, respectively. They were 2620/2600 and 2625/2600 in our experiments.

2.4. Cl^- and calcein permeation

Cl^- permeability was determined by electrometric measurement of Cl^- efflux into $NaNO_3$ solution using an Ionalyer (Orion Research, Model 701A, USA) with a Cl^- selective solid membrane electrode [20]. The buffer solution used was usually composed of 250 mM NaCl/20 mM TES buffer (pH 7.0). The vesicles were separated from untrapped Cl^- by gel permeation chromatography using a Sephadex G-75 gel (0.5×10 cm column) equilibrated with an isotonic buffer, $NaNO_3$/250 mM TES buffer (pH 7.0). The first potentiometric measurements were carried out 10 min for SUV and 7 min for the extruded vesicles after the chromatograph separation had begun.

The measurement of calcein permeation from the vesicles was carried out in 100 mM calcein/20 mM TES buffer (pH 7.0; 388 mOsm), in which the fluorescence intensity of calcein is self-quenched. The vesicles were separated from untrapped calcein by gel permeation chromatography using a Sephadex G-75 gel (0.5×10 cm column) equilibrated with an isotonic buffer, glucose/20 mM TES buffer (pH 7.0). The osmolarity of the buffer was monitored with an Osmometer (Semi-micro Osmometer, Knauer, Germany). The separated vesicles, suspended in a cold isotonic buffer, were rapidly diluted (1:200) into the well-stirred isotonic buffer equilibrated to the experimental temperature. Calcein permeation was detected as an increase in fluorescence intensity.

If Cl^- and calcein permeation obey first-order kinetics:

$$\ln(C_\infty - C_t) = \ln(C_\infty - C_0) - kt \quad (2)$$

where k is the rate constant for permeation of Cl^- or calcein, C_t is the measured concentration at time t, C_0 is the initial concentration, and C_∞ is the concentration after complete liberation of entrapped Cl^- or calcein attained by adding Triton X-100. k is calculated as the slope of the line obtained by plotting $\ln(C_\infty - C_t)$ against t.

The permeability coefficient (p) for Cl^- was obtained from the relation

$$p/k = \text{(internal volume/vesicle)/(membrane area/vesicle)} \quad (3)$$

2.5. Gel permeation chromatography

The vesicle suspensions were prepared in 20 μM of a calcein solution by extrusion and then separated by gel permeation chromatography through a Sephacryl S-1000 (Pharmacia Biotech, Sweden) column (48×1 cm). The lysoPC solution and the sample suspension were, respectively, passed previously through the column many times to make gel saturated with the phospholipids. The total volume and void volume of the column were 19.52 ml and 9.01 ml, respectively. The elution rate was 0.1 ml s^{-1}. The phospholipid recovery was examined based on lipid phosphate that was determined according to Ames [21].

2.6. ^1H NMR measurement

^1H NMR spectra were recorded on a JNM-LA 400WB spectrometer (JEOL, Japan) operating at a radio frequency of 400 MHz. A 45° flip angle (corresponding to a radio frequency pulse of 5 μs) with a repetition rate of 3 s was used. Sodium 3-(trimethylsilyl) propionate-2,2,3,3,-d_4 was used as an internal standard. When the shift reagent $Pr(NO_3)_3$ or lysoPC solution was added to the vesicle suspension, the NMR measurements were carried out within 1 h after the addition. All experiments were carried out at 26°C. The spectra were fitted to Lorenzian lineshapes using the Levenberg–Marquardt method.

3. Results

3.1. Characterization of the PE/lysoPC vesicles

Fig. 1 demonstrates the negatively stained electron micrographs of the extruded (A) and ultrasonicated (B) PE/lysoPC suspensions. Although repeated extrusion appeared to produce more uniform liposomes, the extruded samples are oligolamellar vesicles. However, ultrasonicated vesicles (Fig. 1B) are small uni-

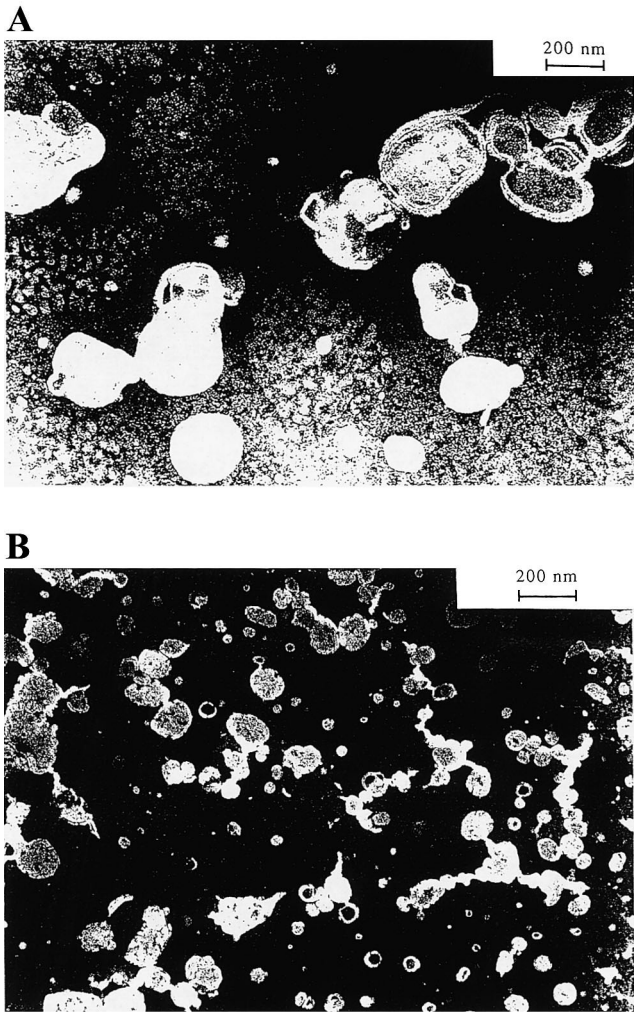

Fig. 1. Negatively stained electron micrographs of the extruded (A) and ultrasonicated (B) PE/lysoPC suspensions.

lamellar ones. Table 1 shows the sizes and calcein entrapment efficiencies of the vesicles. When the molar ratio of PE and lysoPC is 5:2 or 5:3, the calcein entrapment efficiencies of MLV and the extruded vesicles are about 16% and 12–15%, respectively, which corresponds to that of the similar phosphatidylcholine (PC) vesicles. Over a 5:4 molar ratio of PE and lysoPC, the calcein entrapment efficiency decreased and at a 10:1 molar ratio PE precipitation was found. The formation of the vesicular phase is apparently a function of lysoPC concentration. Additionally, no change in either entrapment efficiency or vesicle size was observed within 3 days, showing that those vesicles are stable.

The permeability coefficients (p) and the rate constants (k) of the PE/lysoPC and PC vesicles are shown in Table 2. The permeability coefficient (p) for the PE/lysoPC (5:2) SUV is about 3.47×10^{-10} cm s^{-1}, corresponding to 5.26×10^{-11} cm s^{-1} for PC SUV. In the case of the extruded vesicles, the rate constants of Cl^- and calcein efflux from the PE/lysoPC vesicles are 3.83×10^{-3} s^{-1} and 1.67×10^{-5} s^{-1}, respectively, close to the respective values of 2.00×10^{-4} s^{-1} and 2.67×10^{-5} s^{-1} for the extruded PC vesicles. Apparently, the PE/lysoPC vesicles have a similar barrier potential to the PC vesicles. Small changes in the permeability with the molar ratio of PE and lysoPC might be due to different membrane behaviors.

3.2. The estimate of the incorporation of PE and lysoPC into the vesicles by gel chromatography

Fig. 2 shows a chromatogram for extruded vesicles of PE/lysoPC = 5:2 (A) and 5:3 (B). The gel chromatography is used to separate the vesicles and micelles based on their difference in size and calcein entrapment. According to the gel filter pattern of extruded vesicles at a PE/lysoPC molar ratio = 5:2 (Fig. 2A), a particle size of about 190 nm was calculated from the elution volume and calcein entrapment was also ob-

Table 1
Sizes and calcein entrapment efficiencies of PE/lysoPC and PC vesicles prepared by vortexing[a] and extrusion

Properties	Preparation	PE:lysoPC				PC
		5:1	5:2	5:3	5:4	
Size (nm)	Vortex	1560	890	920	890	950
	Extrusion	189	192	196	183	188
Calcein entrapment (%)	Vortex	11.32 ± 1.16	15.89 ± 2.39	15.63 ± 3.65	6.52 ± 2.68	14.32 ± 2.31
	Extrusion	10.65 ± 3.12	14.68 ± 4.02	12.56 ± 2.13	5.31 ± 2.23	11.78 ± 1.89

[a]Dispersing PE in buffer by adding lysoPC at low temperature, followed by incubating at 37°C.

served. In Fig. 2B (PE/lysoPC molar ratio = 5:3) the elution pattern consists of two peaks, in which the larger one is a characterized vesicle pattern and the smaller one is clearly a micelle pattern because of its small size and no calcein entrapment. Because a high phospholipid recovery was made between 85 and 92%, it was estimated that the 5:2 molar ratio of PE/lysoPC could be incorporated into the vesicles and the increase of lysoPC led to the coexistence of vesicles and micelles.

3.3. The lysoPC behavior in the PE/lysoPC bilayer by ^1H NMR spectroscopy

Fig. 3 shows an expansion of the *N*-methyl (NMe) signal of ^1H NMR spectra for PC SUV (diameter 38 nm) (A), for PE/lysoPC (5:2) SUV (diameter 35 nm) (B) and for PE/lysoPC SUV when lysoPC was added to the PE/lysoPC (5:2) SUV (C). The spectrum of PE/lysoPC SUV, Fig. 3B, a, has the characteristic two NMe signals as a result of packing differences between the internal and external monolayers like PC vesicles, Fig. 3A, a, in which the high-field and low-field signals correspond to the internal and external NMe bands, respectively [22]. A chemical shift separation of 0.021 ppm (8.5 Hz at 400 MHz) for the two NMe signals was observed. The integrated area ratio of the respective NMe signals determined the external to internal molar ratio of PC. For the PC SUV it is 2.94, approximate to the result reported by Brouillette et al. [22], while for PE/lysoPC SUV the lysoPC ratio is 4.05. Apparently, lysoPC preferred the external location. The addition of a shift reagent such as Pr^{3+} results in two discrete NMe resonances, as shown in Fig. 3A,B. Pr^{3+} addition decreased the ratios of the integrated area, 3.89 for PE/lysoPC vesicles and 2.54 for PC vesicles.

As shown in Fig. 3C, the addition of lysoPC to the PE/lysoPC vesicles (5:2 molar ratio of PE:lysoPC) hardly affected the internal NMe resonance, including its chemical shift. On the other hand, the downfield shift of the low-field signal was presumably due to a rapid exchange of lysoPC between the micelles and external monolayer of the vesicles, since the NMe signals were observed at 3.132 ppm for the lysoPC micelles and 3.121 ppm for the external monolayer of the PE/lysoPC vesicles in this experiment, which agrees with the coexistence of the vesicles and micelles in Fig. 2B.

4. Discussion

The vesicle system of PE and lysoPC was judged from the negatively stained electron micrographs in Fig. 1 and the latency of calcein fluorescence in Table 1. In our experiment, the extruded vesicles were found to be oligolamellar ones. Furthermore, the PE/lysoPC membrane was characterized through its barrier potential for Cl^- or calcein efflux. The permeability coefficient (p) is related to the surface area of the unilamellar bilayer. So, it is suitable for the barrier potentials of SUV for Cl^- efflux, but not for the extruded vesicles. However, the difference in the rate constants for the efflux from the vesicles prepared by the same method could reflect the relative comparison of their barrier potential [23]. Therefore, according to the results in Table 2, the barrier potential of the PE/lysoPC vesicular membrane could be totally comparable with the PC membrane.

Chernomordik and Zimmberg have pointed out that molecules with a cone shape, such as PE, caused the negative curvature in phospholipid bilayer like the stalk structures [24]. Siegel has proposed a model for the PE transition of $L_\alpha \rightarrow H_{II}$ under physiological conditions, in which the inverted micellar intermedi-

Table 2
The permeation of Cl^- and calcein from the PE/lysoPC and PC vesicles

Vesicles	Permeation	PE:lysoPC				PC
		5:1	5:2	5:3	5:4	
Extruded vesicles	k (s^{-1}) for Cl^-	1.16×10^{-3}	3.83×10^{-3}	4.07×10^{-3}	4.67×10^{-3}	2.00×10^{-4}
	k (s^{-1}) for calcein	2.67×10^{-5}	1.67×10^{-5}	1.50×10^{-5}		2.67×10^{-5}
Sonicated vesicles	k (s^{-1}) for Cl^-	8.90×10^{-4}	9.62×10^{-4}	6.00×10^{-4}	8.15×10^{-4}	1.08×10^{-4}
	p (cm s^{-1}) for Cl^-	3.58×10^{-10}	3.47×10^{-10}	2.04×10^{-10}	3.72×10^{-10}	5.26×10^{-11}

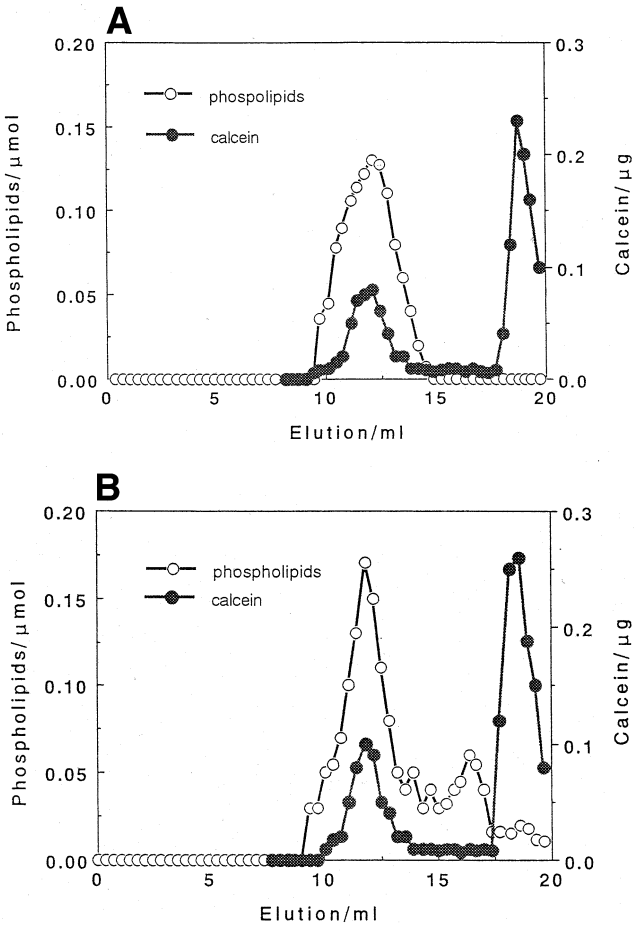

Fig. 2. Fractionation of PE/lysoPC vesicles containing PE:lysoPC molar ratios of 5:2 (A) and 5:3 (B).

ate structure led to the interlamellar attachment [7]. In this study, the formation of PE/lysoPC vesicles upon adding lysoPC solution to the PE lamellar phase at low temperature, followed by incubating this mixture of PE and lysoPC under physiological conditions, indicated that lysoPC was able to block spontaneously the interbilayer attachment. The barrier potential of PE/lysoPC membranes corresponding to PC vesicles, as shown in Table 2, showed a close lamellar molecule packing in the PE/lysoPC vesicles.

^{1}H NMR measurement (Fig. 3B) showed that the external to internal lysoPC ratio is 4.05 for PE/lysoPC SUV, suggesting that lysoPC dominates the external monolayer. Huang et al. reported quantitatively the geometric packing constraints of the vesicle, indicating that the molecule with the inverted cone shape was suitable for the external monolayer and the molecule with the cone shape for the internal monolayer [25]. Marsh has suggested that a bending of the bilayer expands and compresses lipids in the external and internal monolayer, giving rise to an additional curvature free energy [26]. Our NMR results further support this shape hypothesis. Assuming lysoPC was incorporated into the PE/lysoPC vesicles, as was examined in Fig. 2A, this result would indicate an asymmetric distribution of lysoPC between external and internal monolayers of the vesicles. Since the small head-group of PE in comparison to the large area occupied by the hydrocarbon chains gives PE molecules an overall cone shape, the location of PE molecules is facilitated in the internal monolayer with negative curvature. On the other hand, lysoPC has an 'inverted cone' shape and therefore its packing is suitable for the external monolayer. The complementarity of dynamic shapes for PE and lysoPC molecules was apparently responsible for the asymmetric distribution. Furthermore, this asymmetric distribution was able to reduce the curvature free energy driving the formation of PE/lysoPC vesicles.

Chromatography has demonstrated that a 5:2 molar ratio of PE/lysoPC was incorporated into the PE/lysoPC vesicles and that vesicles and micelles coexisted in the 5:3 molar ratio of PE/lysoPC, as shown in Fig. 2. When the lysoPC solution was added to the PE/lysoPC (5:2) vesicle suspension, NMR spectra in Fig. 3C showed that the chemical shift in the high-field peak hardly changed with the additional lysoPC and the NMe resonance in the internal monolayer did not disappear, even with a five-fold addition of the incorporated lysoPC, as illustrated by spectrum c in Fig. 3C, indicating that the vesicle structure was not destroyed by a large amount of added lysoPC. This suggested further that the PE/lysoPC vesicles and micelles could coexist. Similar behavior was also observed when a large amount of lysoPC was added to the PC vesicles [27]. Comparing spectrum a in Fig. 3B with spectra a and b in Fig. 3C, the very small high-field integrated area relative to the low-field one revealed a limit on the amount of lysoPC that could be accommodated in the internal monolayer of the PE/lysoPC vesicles. In other words, the additional lysoPC could not affect the structure of the internal monolayer greatly. This is contrast

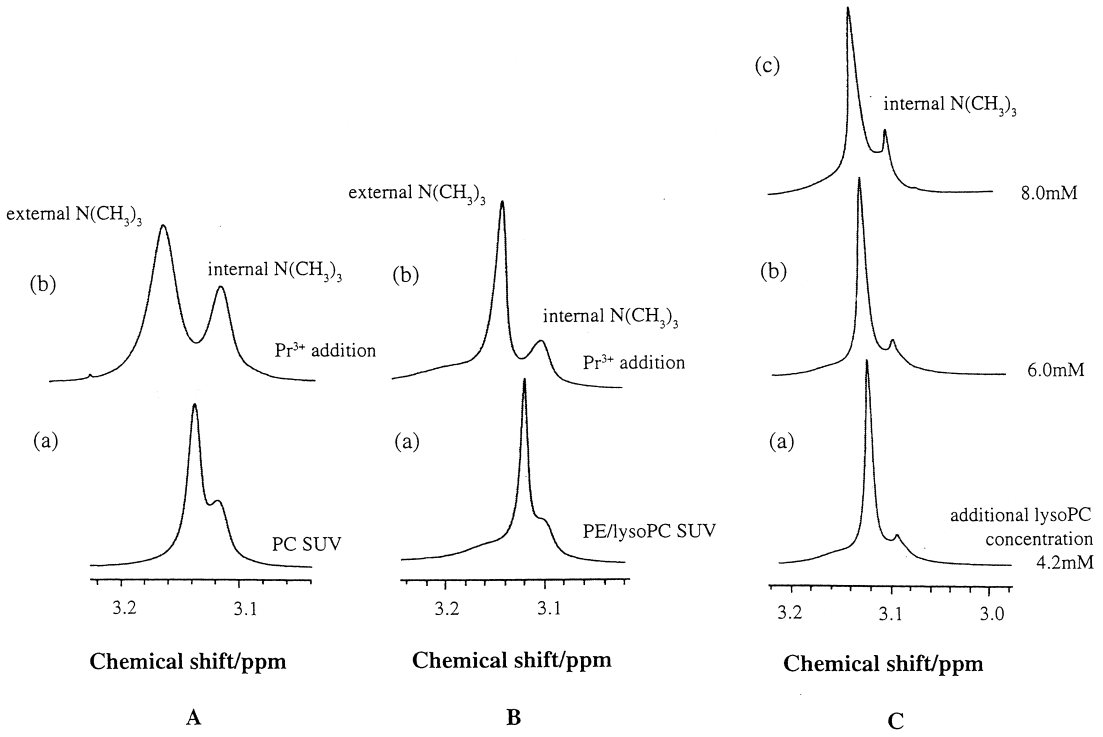

Fig. 3. ^{1}H NMR spectra of NMe signals for ultrasonicated SUV after 24 h equilibration. PC SUV (A), PE/lysoPC SUV (PE:lysoPC = 5:2) with Pr^{3+} (a) and without Pr^{3+} (b) (B), and PE/lysoPC SUV (PE:lysoPC = 5:2) in the case of additional lysoPC 4.2 mM (a), 6.0 mM (b) and 8.0 mM (c) (C).

with the results from PC/sodium deoxycholate mixed vesicles, in which the addition of sodium deoxycholate damaged first the internal monolayer, resulting in vesicle destruction [21]. So, keeping the internal monolayer is very important for vesicle structure. On the other hand, with increasing concentration of the additional lysoPC the low-field signal, which is assigned to the NMe band of the external monolayer, had a down-field shift and its peak area was increased greatly relative to the high-field signal. Those observations were presumably due to a rapid exchange of lysoPC between the external monolayer and micelles, since the vesicles and micelles coexisted when the molar ratio of PE/lysoPC was more than 5:3, as illustrated in Fig. 2B, and the low-field signals in Fig. 3C were the peaks with a narrow half-width. Similar behaviors of lysoPC have been found in the POPC/lysoPC SUV. Kumar et al. have reported that lysoPC preferred the external monolayer of the POPC/lysoPC bilayer and with increasing incorporation of lysoPC the ^{31}P spin–spin relaxation time (T_2*) of the lysoPC in the external monolayer decreased [28]. In addition, Fig. 4 shows the change in the chemical shift separation between the low- and high-field signals when lysoPC was added to the PE/lysoPC vesicle suspension. It can be seen that the chemical shift separation increased, followed by keeping a constant with additional lysoPC con-

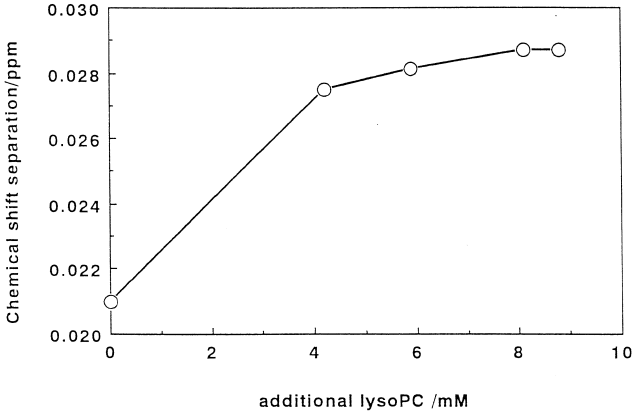

Fig. 4. The chemical shift separation when lysoPC solution was added to PE/lysoPC vesicles (PE:lysoPC = 5:2).

centration. Since the chemical shift separation indicated the difference in the chemical environments or the head-group packing density of lysoPC between the internal and external monolayers of the vesicles [21], the increase in the chemical shift separation implied that the intra-bilayer free energy was increasing, which might be caused by a loose molecular packing in the external monolayer. No further change in the chemical shift separation might imply an exchange equilibrium if a rapid exchange of lysoPC between the micelles and the external monolayer was presented. The different influence of lysoPC on internal and external structures of the vesicles further supports the shape hypothesis, that is, the molecular shape of lysoPC is suitable dynamically for the external monolayer.

Here, either the formation of the PE/lysoPC vesicles or the inhibition of stalks by lysoPC is associated dynamically with the shapes of the component molecules. We considered the behaviors of lipids in terms of their dynamic shapes. PE has the polar head of ethanolamine and two alkyl chains, while lysoPC has choline as a polar head in addition to an alkyl chain. Actually, the hydrophilic and hydrophobic balance of lipid molecules is in structure responsible for their dynamic 'shapes'.

It is accepted that fusion proteins or peptides interact with the PE lipid of the target membrane, producing hexagonal lipid structures of negative curvature, or stalk structures [12], which lower the free energy of membrane fusion [24]. Further, it was found that a variety of widely different fusion events, such as intermicrosome fusion, exocytotic fusion, and baculovirus fusion, were associated with the formation of stalks [29]. On the other hand, inhibition of those fusions in the presence of lysoPC has also been related to the inhibition of stalks by lysoPC [16,17]. The investigations of stalk inhibition by lysoPC were carried out mostly based on the fusion of vesicles with influenza virus. The PE/lysoPC vesicles could act as a model to obtain more information about the inhibition of stalks by lysoPC. In this study, the PE/lysoPC mixture can form a vesicle under physiological conditions, indicating that lysoPC addition results in an easy bilayer structure of PE/lysoPC. Furthermore, the high barrier potential of the PE/lysoPC bilayer similar to PC vesicles showed a tight and stable molecule packing, which may play an important role in the inhibition of a stalk. Otherwise, the coexistence of the vesicles and micelles makes it complicated to elucidate the inhibition of the fusion between influenza virus and vesicles by lysoPC, which could include both inhibition of the stalk and solubilization of the influenza protein by lysoPC [30].

References

[1] J.N. Israelachvili, Biochim. Biophys. Acta 469 (1977) 221–225.
[2] P.R. Cullis, B. De Kruijff, Biochim. Biophys. Acta 559 (1979) 399–420.
[3] D.C. Litzinger, L. Huang, Biochim. Biophys. Acta 1113 (1992) 201–227.
[4] S. Channareddy, S.S. Jose, N. Janes, J. Am. Chem. Soc. 119 (1997) 2345–2347.
[5] J. Navarro, M. Toivio-Kinnucan, E. Racker, Biochemistry 23 (1984) 130–135.
[6] D.P. Siegel, Biophys. J. 49 (1986) 1155–1170.
[7] D.P. Siegel, Biophys. J. 65 (1993) 2124–2140.
[8] L.V. Chernomordik, G.B. Melikyan, Y.A. Chizmadzhev, Biochim. Biophys. Acta 906 (1987) 309–352.
[9] M.M. Kozlov, V.S. Markin, Biofizika 28 (1983) 255–261.
[10] P.E. Glaser, R.W. Gross, Biochemistry 33 (1994) 5805–5812.
[11] H. Ellens, D.P. Siegel, D. Alford, G.L. Yeagle, L. Boni, L.J. Lis, P.J. Quinn, J. Bentz, Biochemistry 28 (1989) 3692–3703.
[12] F.M. Goni, J.L. Nieva, G. Basanez, G. Fidelio, A. Alonso, Biochem. Soc. Trans. 22 (1994) 839–844.
[13] K. Gawrisch, V.A. Parsegian, D.A. Hajduk, M.W. Tate, S.M. Gruner, N.L. Fuller, R.P. Rand, Biochemistry 31 (1992) 2856–2864.
[14] P.L. Yeagle, F.T. Smith, J.E. Young, T.D. Flanagan, Biochemistry 33 (1994) 1820–1827.
[15] R.M. Epand, R.F. Epand, N. Ahmed, R. Chen, Chem. Phys. Lipids 57 (1991) 75–80.
[16] A. Helenius, D.R. McCaslin, E. Fries, C. Tanford, Methods Enzymol. 1 (1979) 734–747.
[17] L.V. Chernomordik, E.A. Leikina, M.-S. Cho, J. Zimmerberg, J. Virol. 69 (1995) 3049–3058.
[18] S.S. Vogel, E.A. Leikina, L.V. Chernomordik, J. Biol. Chem. 268 (1993) 25764–25768.
[19] N. Oku, D.A. Knedall, R.C. Macdonald, Biochim. Biophys. Acta 691 (1982) 332.
[20] M. Ueno, Biochim. Biophys. Acta 904 (1987) 140–144.
[21] B.N. Ames, Methods Enzymol. 8 (1966) 115–117.
[22] C.G. Brouillette, J.P. Segrest, T.C. Ng, J.L. Jones, Biochemistry 21 (1982) 4569–4575.
[23] K. Anzai, H. Utsumi, K. Inoue, S. Nojima, T. Kwan, Chem. Pharm. Bull. 28 (1980) 1762–1770.

[24] L.V. Chernomordik, J. Zimmerberg, Curr. Opin. Struct. Biol. 5 (1995) 541–547.
[25] C. Huang, J.T. Mason, Proc. Natl. Acad. Sci. USA 75 (1978) 308–310.
[26] Marsh (1996) Biochim. Biophys. Acta 1286, 183–223.
[27] S.P. Bhamidipati, J.A. Hamilton, Biochemistry 34 (1995) 5666–5677.
[28] V.V. Kumar, B. Malewicz, W.J. Baumann, Biophys. J. 55 (1989) 789–792.
[29] L.V. Chernomordik, S.S. Vogel, A. Sokoloff, H.O. Onaran, E.A. Leikina, J. Zimmerberg, FEBS Lett. 318 (1993) 71–76.
[30] S. Gunther-Ausborn, A. Praetor, T. Stegmann, J. Biol. Chem. 270 (1995) 29279–29285.